http://doi.org/10.35784/iapgos.3376 *received: 16.05.2022 | revised: 02.09.2022 | accepted: 15.12.2022 | available online: 30.12.2022*

SCATTERING BY CIRCULAR VOIDS WITH RIGID BOUNDARY: DIRECT AND INVERSE PROBLEMS FOR OPEN AND CLOSE DOMAINS

Tomasz Rymarczyk[1,2], Jan Sikora[1,2]
[1]Research & Development Centre Netrix S.A., Lublin, Poland, [2]WSEI University, Faculty of Transport and Informatics, Lublin, Poland

Abstract*. Problems with the accuracy of calculations by the Boundary Element Method of acoustic and ultrasonic problems formulated in the frequency domain were presented in this paper. The inverse problem was formulated to identify the position and dimensions of the scattering object. A series of numerical experiments carried out with the help of the Boundary Elements Method proved the algorithm's robustness to noise and high precision in a wide frequency spectrum.*

Keywords: acoustics-ultrasound wave propagation, BEM simulation, inverse problems, optimization methods

ROZPRASZANIE PRZEZ PUSTE PRZESTRZENIE KOŁOWE ZE SZTYWNĄ GRANICĄ: PROSTE I ODWROTNE ZAGADNIENIA DLA OBSZARÓW OTWARTYCH I ZAMKNIĘTYCH

Streszczenie. *W pracy przedstawiono problemy z dokładnością obliczeń Metodą Elementów Brzegowych zagadnień akustycznych i ultradźwiękowych sformułowanych w dziedzinie częstotliwości. Sformułowano zagadnienie odwrotne dla identyfikacji położenia i wymiarów obiektu rozpraszającego. Seria eksperymentów numerycznych przeprowadzonych z pomocą Metody Elementów Brzegowych udowodniła odporność algorytmu na szum oraz wysoką precyzję w szerokim spektrum częstotliwości.*

Słowa kluczowe: propagacja fal akustycznych-ultradźwiękowych, symulacja Metodą Elementów Brzegowych (MEB), zadania odwrotne, metody optymalizacyjne

Introduction

The key problem of each inverse problem is the forward problem. This paper deals with the accuracy and effectiveness of calculating the acoustic and ultrasound forward problem. Very often, Ultrasound terminology is used interchangeably with Ultrasonic. What is the difference, then? In practice, ultrasound is used to reference clinical ultrasonic scanning and therapeutic ultrasound imagery, but Ultrasonic refers to technical imagining, for example, Non-Destructive Testing. We will use the acoustic waves in the acoustic and ultrasound ranges.

Briefly, we introduce two types of problems frequently occurring in practical applications. First, problems of wave propagation phenomena are usually classified as interior or exterior, depending on whether one is interested in the sound field in bounded or unbounded regions in space. In some cases, the third type of acoustic problem could also be defined when the domain of interest is not simply connected (see for example Fig. 5). The last one is often called the hybrid interior-exterior problem [4].

This paper focuses readers' attention on the BEM for hybrid interior-exterior problems formulated for the frequency domain.

Based on the Forward Problem, Dedicated iterative methods make it possible to formulate the inverse problems and solve the tomography tasks for acoustic [3, 4, 6]. The advantages of the acoustic or ultrasound approach for imaging, particularly in medicine, are obvious and do not demand further explanations.

Ultrasound tomography models, especially for the integral formulation, are difficult from a numerical point of view [4].

1. Point source

Why are we interested in problems related to point-generated wave fields? It has several reasons. The more important one is due to the variety of applications coming from the theory of composite materials and acoustic emission, from the theoretical analysis of biological studies at the cell level, from non-destructive testing and evaluation, from geophysics, and from modelling in medicine and health sciences. Furthermore, a point-source field is more easily realizable in a laboratory [2].

Suppose that our incoming wave is of point source form, with the source at r' illuminating the circular cylinder surface cross-section defined in terms of the incident angles (ψ_0,θ_0), as illustrated in Fig. 1a.

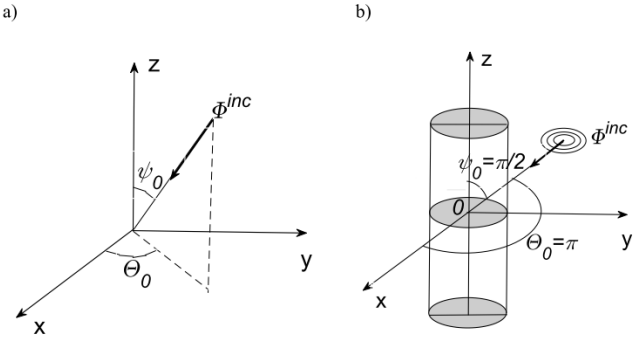

Fig. 1. Time-harmonic wave a) with an arbitrary incident angle (ψ_0,θ_0), b) scattering from a circular cylinder with an incident angle ($\theta_0 = \pi$)

Located the source point on the surface x0y (angle $\psi_0 = \pi/2$) and for angle $\theta_0 = \pi$ as is shown in Fig. 1b, the total field satisfies the Helmholtz equation (1).

The acoustic field is assumed to be present in the domain of a homogeneous isotropic fluid, and it is modelled by the linear wave equation [4]:

$$\nabla^2\psi(\mathbf{p},t) = \frac{1}{c^2}\frac{\partial^2}{\partial t^2}\psi(\mathbf{p},t) + Q \tag{1}$$

where $\psi(\mathbf{p},t)$ [m^2/s] is the scalar time-dependent velocity potential related to the time-dependent particle velocity $\mathbf{v}(\mathbf{p},t) = \nabla\psi(\mathbf{p},t)$ [m/s] and c [m/s] is the propagation velocity ($\mathbf{p}$ and t are the spatial and time variables in meters and seconds respectively). The time-dependent sound pressure is equal $p(\mathbf{p},t) = -\rho\frac{\partial}{\partial t}\psi(\mathbf{p},t)$ where ρ [kg/m^3] is the density of the acoustic medium.

Transferring from the time domain to the frequency domain, the velocity potential ψ can be expressed as follows:

$$\Psi(\mathbf{p},t) = \mathrm{Re}\{\varphi(\mathbf{p})\mathrm{e}^{-\mathrm{i}\omega t}\}, \tag{2}$$

where: $\omega = 2\pi f$ [1/s] and $\varphi(\mathbf{p})$ is the velocity potential amplitude. The substitution of the above expression into the wave equation reduces it to the Helmholtz equation of the form [4]:

$$\nabla^2\varphi(\mathbf{p}) + k^2\varphi(\mathbf{p}) = Q, \tag{3}$$

where $k^2 = \frac{\omega^2}{c^2}$ is the wave number and the wavelength is equal to $\lambda = c/f$. The right-hand side Q stands for the acoustic source. The complex-valued state function $\varphi(\mathbf{p})$ possess the magnitude and phase shift.

The problem is outlined by beginning with the time-harmonic reduction of the wave equation for the exterior-interior problem to the Helmholtz equation (Eq. 3) and finally to the Boundary Integral Equation formulation for the acoustic scattering problem.

The sound-hard scatterer is imposed on the interior and exterior boundary through a homogeneous Neumann boundary condition. Making use of Green's second identity, the Helmholtz equation can be expressed in an equivalent form of a Boundary Integral Equation (BIE) [4], i.e.

$$c(\boldsymbol{r})\varphi(\boldsymbol{r}) + \int_{\Gamma} \frac{\partial G(|\boldsymbol{r}-\boldsymbol{r}'|)}{\partial n}\varphi(\boldsymbol{r}')d\boldsymbol{\Gamma} = \\ = \int_{\Gamma} G(|\boldsymbol{r}-\boldsymbol{r}'|)\frac{\partial\varphi(\boldsymbol{r}')}{\partial n}d\boldsymbol{\Gamma} + \varphi^{inc}(\boldsymbol{r}), \quad \boldsymbol{r}\in\boldsymbol{\Gamma} \tag{4}$$

where φ^{inc} is the incident wave, and the vector $\boldsymbol{n}$ is the normal unit vector outward pointing from the considered domain.

Due to the homogeneous Neumann boundary conditions, the third term of Eq. (4) vanishes. So now the integral boundary equation (4) for constant boundary elements can be written in terms of local coordinate ξ as follows:

$$c(\boldsymbol{r})\varphi(\boldsymbol{r}) + \sum_{j=1}^{M}\varphi_j(\boldsymbol{r}')\int_{-1}^{+1}\frac{\partial G(|\boldsymbol{r}-\boldsymbol{r}'|)}{\partial n}J(\xi)d\xi = \varphi^{inc}(\boldsymbol{r}) \tag{5}$$

where: M – is the total number of constant elements and $J(\xi)$ – is the Jacobian of transformation $\left(J(\xi) = \frac{d\boldsymbol{\Gamma}}{d\xi} = \right.$ $\left. = \sqrt{\left(\frac{dx(\xi)}{d\xi}\right)^2 + \left(\frac{dy(\xi)}{d\xi}\right)^2} = \frac{L}{2}\right)$, where L is the length of the constant boundary element [7, 9].

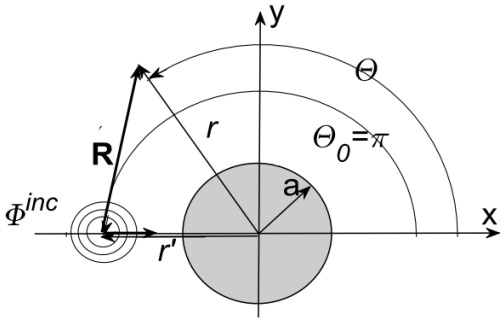

Fig. 2. Diagram showing the circular scatterer due to a point source located at r' at angle $\theta_0 = \pi$ calculated from the positive direction of x axis

Then, the fundamental solution for the field at **r** is given by:

$$\varphi^{inc}(r,\theta) = \frac{i}{4}H_0^{(1)}(kR) \tag{6}$$

where $R = |\mathbf{R}| = |\mathbf{r}-\mathbf{r}'|$, as seen in Fig. 2. The incoming wave described by Eq. (6) using the Graf's addition formula [5] can be expanded as follows:

$$\varphi^{inc}(r,\theta) = \frac{i}{4}H_0^{(1)}(kr')J_0(kr) + \\ + \frac{i}{4}\sum_{n=1}^{\infty}2\,(-1)^n H_n^{(1)}(kr')J_n(kr)\cos\big(n(\theta-\theta_0)\big) \tag{7}$$

Then, we can expand our scattered field in the following form:

$$\varphi^{scat}(r,\theta) = A_0H_0^{(1)}(kr) + \\ + \sum_{n=1}^{\infty}2\,(-1)^n A_nH_n^{(1)}(kr)\cos\big(n(\theta-\theta_0)\big) \tag{8}$$

The amplitude of the n-th mode for the Neumann boundary conditions will be:

$$A_n = -\frac{i}{4}\frac{H_n^{(1)}(kr')\,J_n'(ka)}{H_n^{(1)\prime}(ka)} \tag{9}$$

$$A_0 = -\frac{i}{4}\frac{H_0^{(1)}(kr')\,J_0'(ka)}{H_0^{(1)\prime}(ka)} \tag{10}$$

where the prime sign denotes derivatives concerning the argument ka and a is the radius of the circular void (see Fig. 2). The first derivatives are calculated according to [1], and we will have:

$$J_0'(ka) = -J_1(ka) \tag{11}$$

$$J_n'(ka) = \frac{1}{2}\big(J_{n-1}(ka) - J_{n+1}(ka)\big) \tag{12}$$

and similarly, for the Hankel functions, we have got:

$$H_0^{(1)\prime}(ka) = -H_1^{(1)}(ka) \tag{13}$$

$$H_n^{(1)\prime}(ka) = \frac{1}{2}\Big(H_{n-1}^{(1)}(ka) - H_{n+1}^{(1)}(ka)\Big) \tag{14}$$

So:

$$A_n = -\frac{i}{4}H_n^{(1)}(kr')\frac{J_{n-1}(ka)-J_{n+1}(ka)}{H_{n-1}^{(1)}(ka)-H_{n+1}^{(1)}(ka)} \tag{15}$$

and

$$A_0 = -\frac{i}{4}H_0^{(1)}(kr')\frac{J_1(ka)}{H_1^{(1)}(ka)} \tag{16}$$

2. Point wave and its asymptotic behaviour

When we do not have the analytic solution to check the BEM solution, we can add one more way of control. The point source generates a spherical wave. When the distance from the scatterer becomes infinitely long, the spherical wave could be treated as the plane wave. For this case exists, the analytic solution [8] so it is possible to compare the point source excitation results qualitatively. If the results are similar, we can get one more reason to ensure that the BEM calculations are correct. Let us consider the point source located in the position (2,0) outside the scatterer of radius a = 1 m (see Fig. 2).

In Fig. 3a and Fig. 3b, we can see that curve of potential distribution on the surface of the circular scatterer in the case of remote point source becomes, regarding the shape, identical to the plane wave shown in Fig. 3c.

Examples presented in figures 3 and 4 fulfil the demand concerning discretization that the number of boundary elements per wavelength should not be less than 10 [4, 9]. In this case, twelve boundary elements per wavelength should guarantee correct results. Additionally, we check the asymptotic behaviour of BEM calculation. The location of the source was moved far away from the scatterer, and the results closely approach the previous ones for the plane wave illumination. However, of course, we can make only a qualitative comparison.

Comparing results presented in Fig. 3b with results in Fig. 3c, the agreement concerning the shape is particularly good. However, the result magnitudes are different because, in both cases, the source amplitudes were equal, but the energy radiated due to the mathematical model was different. On this basis, we can state that the BEM model provides correct results.

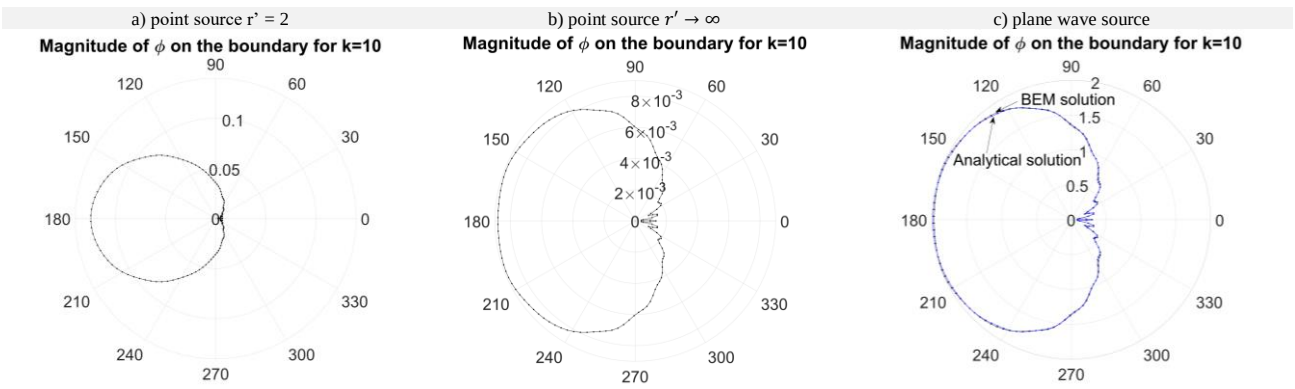

Fig. 3. The circular scatterer illuminated by: a) point source located close to the scatterer, b) source point located far away from the scatterer when the radius $r' \to \infty$, c) plane wave source

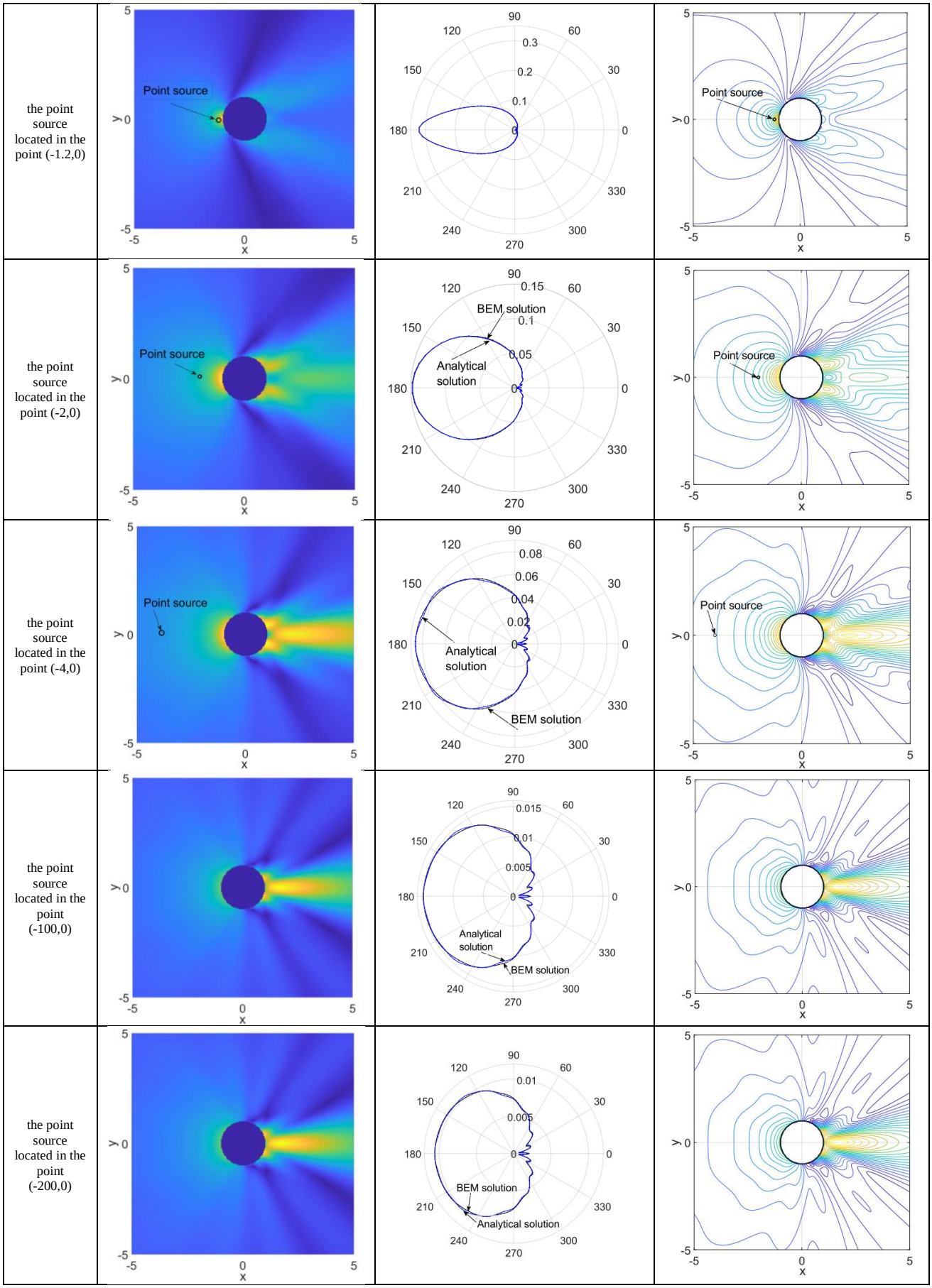

Fig. 4. Position of the point source (first column), the image of the acoustic field (second column), distribution of the acoustic velocity potential on the perimetry of the circular scatterer (third column) and equipotential lines of the velocity potential (fourth column), when the scatterer is illuminated by the point source placed in various locations

3. The inverse acoustic problem

The first part of the paper is devoted to precisely calculating the forward problems in acoustic or ultrasonic. Ultra-sound is a branch of acoustics with soundwave frequency above 20 kHz that utilize the mechanical pressure wave above the human hearing range.

This part could be treated as preparation and a benchmark for point sources used in the scattering acoustic/ultrasound problems. The BEM was selected as the most popular and effective for the open boundary problem so frequently encountered in Acoustic theory. The benchmark was needed due to a high argument of the Green functions (the Helmholtz function) and an integration of the singular integrands in BEM [4]. The first part of the paper proved that BEM could deal with both difficulties and provide a precise result. Moreover, some useful criteria for Inverse Problems in Acoustic or Ultrasound were formulated based on analytical results. In this paper, we would like to focus readers' attention on the BEM formulated for the frequency domain (see Eq. 3). Formally, the mathematical description would be almost identical as for Diffuse Optical Tomography [6–9], but the physical meaning of the state function, material coefficient and their units are different.

The idea of the inverse problem in the transmission mode is sketched in Fig. 5, where the signal is transmitted as a fan-shaped beam by the transducer and received by the opposite sensors acting as the receivers (see Fig. 5).

In the transmission mode of Acoustic/Ultrasonic Tomography (AT), we may compare the pulses' amplitudes measured on the external boundary's perimetry (see Fig. 6) to image the scatterer within the region.

The idea of the inverse problem in the transmission mode is sketched in Fig. 5, where the signal is transmitted as a fan-shaped beam by the transducer and received by the opposite sensors acting as the receivers (see Fig. 5).

In the transmission mode of Acoustic/Ultrasonic Tomography (AT) we may compare the amplitudes of the pulses measured on the perimetry of the external boundary (see Fig. 6) to image the scatterer within the region.

Application of the Boundary Element Method to solve the forward problem implies some simplified assumptions regarding imaging in AT. First, the BEM is designed for homogeneous region analysis only. So, in this case, imaging will be restricted to the dimensioning and location problem, a special case of the Optimal Shape Design problem. It means that the image would be parametrized. As a result, we will have only three parameters: namely, the scatterer's radius and two parameters (length and angle) for the position vector. For the scattering problems, such an approach is particularly justified [7].

4. The acoustic tomography

In tomography, we have only access to the external boundary to make the measurements. So, the number of measured data is strongly limited. To enlarge them successfully, the point source position is changed, illuminating the scatterer from different angles. The source positions are called the Projection Angles (PA). In that way, the number of measurements is multiplied by the number of Projection Angles (see Fig. 5).

The crucial point of an Inverse Problem is the Sensitivity Analysis, which is particularly difficult for BEM [4]. So, to avoid the Sensitivity Analysis for BEM being complicated and time-consuming, the **fmincon** function was selected [10, 11]. This function can effectively find a minimum of a constrained nonlinear multivariable function.

5. Definition of the objective function

To match the signal calculated in each iteration step to the measured one, the following objective function has been defined Eq. (17). The analysis was carried out in the frequency domain, which means that all signals are complex, having magnitude and phase shift.

This objective function will be subject to minimization with linear inequality constraints:

$$\hat{\Phi} = \sum_{j=1}^{j=p} \hat{\Phi}_j = \sum_{j=1}^{j=p} \left(\hat{f}_j - \hat{v}_{0j}\right) = \left(\hat{\mathbf{F}} - \hat{\boldsymbol{V}}_0\right) = \\ = \sum_{j=1}^{j=p} \mathrm{Re}\left(\hat{f}_j - \hat{v}_{0j}\right) + j \sum_{j=1}^{j=p} \mathrm{Im}\left(\hat{f}_j - \hat{v}_{0j}\right) \qquad (17)$$

where: hat means a complex quantity, $\hat{\Phi}$ – global auxiliary complex function calculated for all $p = 8$ or 16 positions of the points source (so-called projection angles), $j = 1, 2\,I\,, p$, $\hat{\Phi}_j$ – auxiliary complex function for the j-th position of the acoustic point source, $\hat{\mathbf{f}}_j$ a vector representing the calculated complex signal for the current iterative step (see, for example, Fig. 6), $\hat{\mathbf{v}}_{0j}$ – vector of measured signal for the j-th position of the point source. The complex matrices $\hat{\mathbf{F}}$ and $\hat{\boldsymbol{V}}_0$ are equal respectively:

$$\hat{\mathbf{F}} = \left[\hat{\mathbf{f}}_1, \hat{\mathbf{f}}_2, \ldots, \hat{\mathbf{f}}_{\boldsymbol{p}}\right]^{\boldsymbol{T}} \text{ and } \hat{\boldsymbol{V}}_0 = \left[\hat{\mathbf{v}}_{01}, \hat{\mathbf{v}}_{02}, \ldots, \hat{\mathbf{v}}_{0\boldsymbol{p}}\right]^{\boldsymbol{T}} \qquad (18)$$

Equation (17) could be shown in the following form:

$$\hat{\Phi} = \sum_{j=1}^{j=p} \hat{\phi}_j = \sum_{j=1}^{j=p} \mathrm{Re}\,\hat{\phi}_j + j \sum_{j=1}^{j=p} \mathrm{Im}\,\hat{\phi}_j. \qquad (19)$$

The objective function must be the real number, so it is defined in a following way:

$$F = \sum_{j=1}^{j=p} \left(\hat{\phi}_j \hat{\phi}_j^*\right) = \sum_{j=1}^{j=p} \left(\mathrm{Re}^2 \hat{\phi}_j + \mathrm{Im}^2 \hat{\phi}_j\right). \qquad (20)$$

where $\hat{\phi}_j^*$ means complex conjugate auxiliary function.

From the physical point of view, the objective function F is a distance in the complex plane between the measured and calculated signal. Minimizing distance means that both signals become as close to each other as possible.

Let us consider a set (array) of acoustic source points (sensors marked by yellow) to achieve the image, as shown in Fig. 5.

The reconstruction of the object (geometry only, without acoustical properties of the material) requires an accurate numerical model [4, 6]. Moreover, it allows us to solve the inverse scattering problem, i.e., determine the parameters of the scatterer based on measurements of the incident and scattered fields taken on the external circular boundary.

Inverse scattering problems are non-linear and ill-posed. Therefore, no single solution exists, and it is necessary to eliminate the solutions that do not correspond to reality.

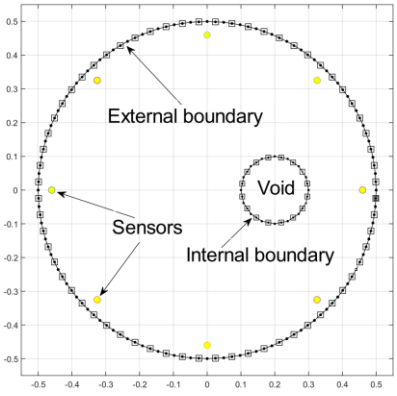

Fig. 5. Sketch of the transmission mode of AT

An example of state function distribution on the external boundary for all projection angles (PA) is shown in Fig. 6. Also, it is interesting to see the image of the acoustic field inside the region for different projection angles.

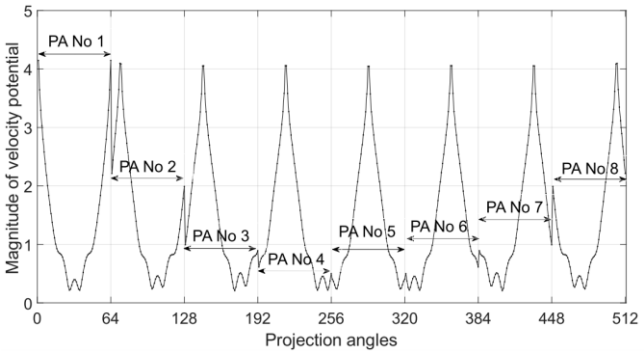

Fig. 6. State function (Velocity potential) distribution along the external boundary of the region for all Projection Angles

It demands of internal field calculations, which are numerically expensive because such numerical integration demands much more integration points compared to boundary integrals [9]. The images of the field are shown in Fig. 7.

6. Definition of inequality constrains

The imagining problem was turned into the optimization problem, which means parametrization of an image. following parameters could sufficiently describe the proposed image: internal radius of the circular void-scatterer r_1, and the position vector of the centre of the scattering object r_2.

During the optimization process, the internal object should not cross the external boundary of the region R_o. All radiuses should have a positive value.

Mathematically those constraints could be expressed as follows:

$$\begin{bmatrix} -1 & 0 \\ 0 & -1 \\ 1 & 1 \end{bmatrix} \begin{bmatrix} r_1 \\ r_2 \end{bmatrix} < \begin{bmatrix} -0.1R_0 \\ 0 \\ 0.9R_0 \end{bmatrix} \tag{21}$$

where: r_1 – radius of the scatterer, r_2 – length of the position vector, R_o – radius of the region to be imaged. The third parameter – an angle of position vector- remains without constraints.

7. Boundary conditions and material properties

The circular cross-section of the scatterer boundary and the boundary of the whole area is rigid. That is why the homogeneous Neumann boundary conditions on both edges were imposed. The air fills the area. The velocity of a sound wave is equal to 344 m/s [4, 6].

8. Result and discussion

The transmission mode and optimization algorithm with linear inequality constraints have been used to reconstruct the image which was parametrized. Transmission mode has the concept of transmitting the velocity potential and, as needed, the pressure signal from the transmitter when the other transducers act as receivers (see in Fig. 5). As shown in figure 5, where the transducer No one is transmitting a continuous sound wave signal and the other transducers are receiving. It is the first PA. Next, the second sensor starts playing the transmitter and sensor role. Then, no 1 becomes the receiver and so on. Such a change in the role of the sensors is named the projection angle. Results of the velocity potential distribution for all the projection angles is presented in Fig. 8. The signal is polluted by the 10% noise (the upper figure) and 20% noise (lower figure). The 20% pollution is really the big one.

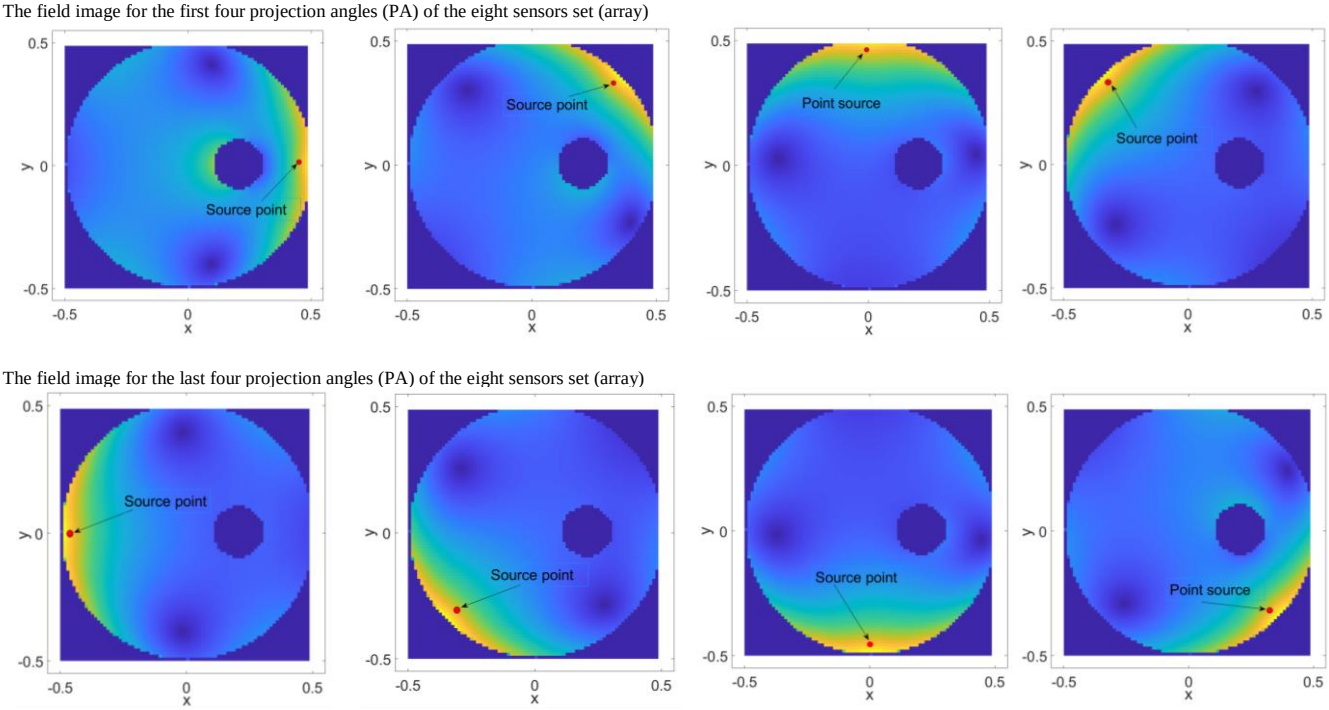

Fig. 7. Eight element array sensors: velocity absolute value distribution for the point source excitation

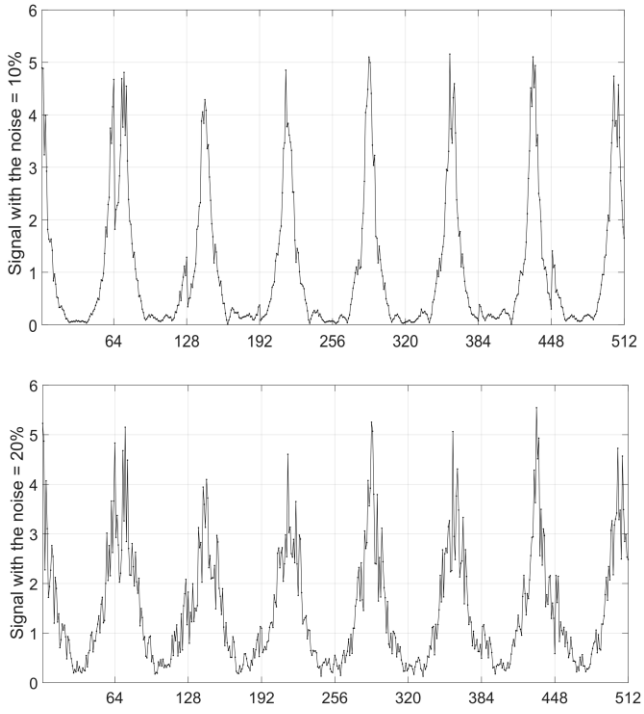

Fig. 8. Synthetic signal treated as the measured one with: a) 10% noise, b) 20% noise for eight projection angles

Numerical simulation was carried out for different geometrical parameters as well as for different frequency from acoustical range (Fig. 9) up to ultrasound range (Fig. 10).

The frequency is an impact factor when dealing with ultrasonic solutions in fluids and air. Therefore, a transducer with greater frequency can resolve objects with smaller dimensions. We can observe this phenomenon in the following figures.

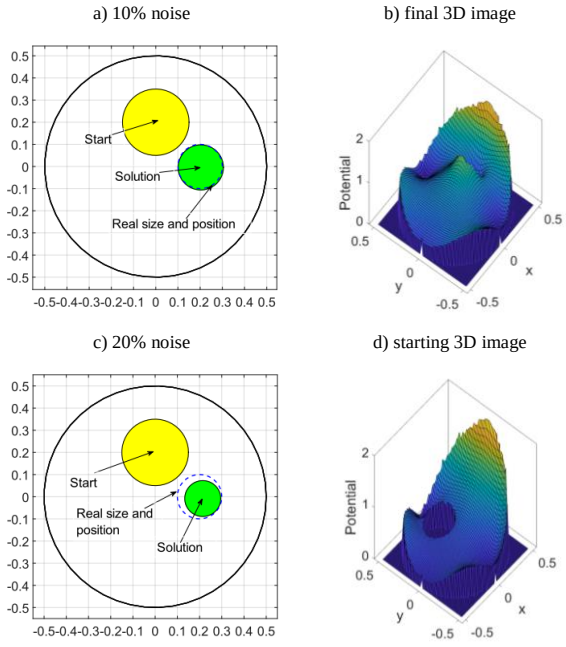

Fig. 9. Inverse problem solution of parametrized image when the measurements are polluted by: a) 10% noise, b) 3D image, c) 20% noise, d) 3D image for the starting point

Fig. 9 presents the inverse solution for the acoustic frequency equal to f = 5.47 kHz and for the wave number k = 1 [1/m].

For the outer boundary circle, the number of boundary elements per lambda wavelength = 128, and for the inner circle, the number of boundary elements per lambda wavelength = 160.

Those numbers are much higher than the discretisation criterion, stating that the number of boundary elements should be bigger than ten boundary elements per acoustic wavelength. Fig. 9 presents the results for 10% and 20% of pollution (left column). In the right column are shown the distribution of the acoustic fields inside the region for final and starting position.

For the 10% of pollution, the maximal error was 8.0% for the radius location and 2.5% for the radius of the scatterer. And for 20% of noise, 19%, and 7.0%, respectively. In the right column are pictures of the field distribution inside the area. In the upper row of this column, the image is for the real position of the scatterer, but the lower row is for the starting position of the optimization process.

The same numerical experiment was carried out for ultrasonic frequency equal to f = 38.30 kHz and the wave number k = 7 [1/m]. The images are presented in Fig. 10. Now, for the external boundary circle, the number of boundary elements per wavelength lambda = 18.3, and for the internal circle number of boundary elements per wavelength lambda = 22.9. This time the number of boundary elements per wavelength is closer to the precision criterion, which means that discretization is more economical from the tomography point of view.

For ultrasound tomography with 10% noise, the maximal error was less than 20% which is unacceptable (see Fig. 10 upper row). However, it is possible to reduce the significant error by enlarging the number of sensors (see Fig. 10, the lower row).

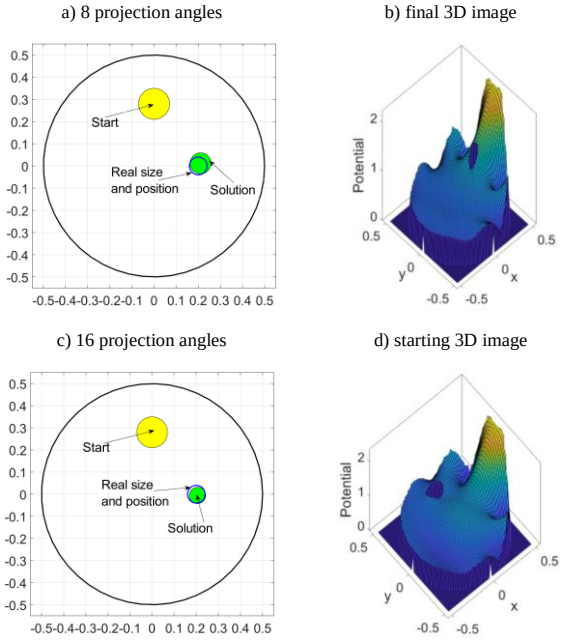

Fig. 10. Synthetic signal treated as the measured one with: a) 10% noise for 8PA, b) 3D field image c) 10% noise but for 16 PA d) 3D image for the starting point

The level of the maximal error for ultrasonic frequency is about twice as much as for the acoustical frequency, as shown in Fig. 11.

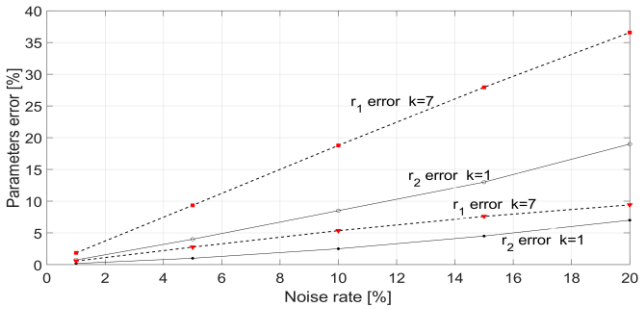

Fig. 11. Relative error as a function of the signal noise rate for two different wave numbers

As shown in figure 11, the error sometimes reaches more than 30%. So, the question is how to reduce the level of the maximal error?

There are at least two ways. One of them is presented in Fig. 10 (the lower row). Namely, the number of sensors doubled. For maximal error reduction, we must pay by the execution time, which is painful for the optimization process. However, it is possible to reach much better results, as seen in Fig. 10. The error was reduced to 7.1% for the radius location and 2.8% for the scatterer radius.

9. Conclusions

From a tomography point of view, the most important is a grid providing a minimum number of points per wavelength to resolve the acoustic or ultrasonic problem even for the highest frequencies. Our goal is ultrasound tomography, so we must consider frequency above 20 kHz. Unfortunately, the wavelength became noticeably short for such frequencies, even less than 0.017 m.

In tomography problems, we often deal with many sensors emitting and receiving signals closely located to the external boundary. For example, Diffuse Optical Tomography or Radio Tomography could be mentioned [5-7].

The literature [1-3] stresses that the acoustic wavelength should be much greater than the length scale of the region under consideration. That means that the ratio of the wavelength to the length of the boundary element should be at least equal to 8-10. Then, we trust that the precision of the calculation will be secured.

However, it might be difficult in tomography to fulfil such rigorous demands. For example, for the ultrasound frequency band, the length of the boundary elements should be extremely small if the error level should be kept at a low level. From the point of view of the Inverse Problem efficiency calculation, such a decision would be difficult to justify. Therefore, some compromise between the accuracy and the execution time must be preserved. In the author's opinion, coarse discretization might be sufficient in some cases.

References

[1] Abramowitz M., Stegun I. A.: Handbook of mathematical functions with formulas, graphs, and mathematical tables. John Wiley, New York 1973.
[2] Athanasiadis C.: Scattering relations for point sources: Acoustic and electromagnetic waves. Journal of mathematical physics 43(11), 2002, 5683.
[3] Harwood A. R. G.: Numerical Evaluation of Acoustic Green's Functions. PhD School of Mechanical, Aerospace & Civil Engineering, University of Manchester, Manchester 2014.
[4] Kirkup S.: The Boundary Element Method in Acoustics: A Survey. Applied Sciences 9(8), 2019, 1642 [http://doi.org/10.3390/app9081642].
[5] Lynott G. M.: Efficient numerical evaluation of the scattering of acoustic and elastic waves by arrays of cylinders of arbitrary cross section. Thesis of Doctor of Philosophy. School of Natural Sciences, Department of Mathematics, University of Manchester, Manchester 2020.
[6] Opieliński K. J., Pruchnicki P., Gudra T.: Ultrasonic Mammography with Circular Transducer Array. Archives of Acoustics 39(4), 2014, 559–568 [http://doi.org/10.2478/aoa-2014-0060].
[7] Rymarczyk T.: Tomographic Imaging in Environmental, Industrial and Medical Applications. Innovatio Press Publishing Hause, Lublin 2019.
[8] Rymarczyk T., Sikora J.: On precision acoustic wave calculation in a frequency domain. IAPGOS 2, 2022, 64–68 [http://doi.org/10.35784/iapgos.2966].
[9] Sikora J.: Boundary Element Method for Impedance and Optical Tomography. Warsaw University of Technology Publishing Hause, Warsaw 2007.
[10] https://www.comsol.com/acoustics-module
[11] https://reference.wolfram.com/language/PDEModels/tutorial/Acoustics/AcousticsFrequencyDomain.html

Prof. D.Sc. Ph.D. Eng. Tomasz Rymarczyk
e-mail: tomasz@rymarczyk.com

He is the director of the Research and Development Centre in Netrix S.A. and the Institute of Computer Science and Innovative Technologies at WSEI University, Lublin, Poland. He worked in many companies and instituted developing innovative projects and managing teams of employees. His research focuses on applying non-invasive imaging techniques, electrical tomography, image reconstruction, numerical modelling, image processing and analysis, process tomography, software engineering, knowledge engineering, artificial intelligence, and computer measurement systems.

http://orcid.org/0000-0002-3524-9151

Prof. D.Sc. Ph.D. Eng. Jan Sikora
e-mail: sik59@wp.pl

Prof. Jan Sikora (PhD. DSc. Eng.) graduated from Warsaw University of Technology Faculty of Electrical Engineering. During 44 years of professional work, he has obtained all grades, including the position of full professor at his alma mater. Since 1998 he has also worked for the Institute of Electrical Engineering in Warsaw. In 2008, he joined Electrical Engineering and Computer Science Faculty in Lublin University of Technology. During 2001-2004 he has worked as a Senior Research Fellow at University College London in the prof. S. Arridge's Group of Optical Tomography. His research interests are focused on numerical analysis application in field theory. He is the author of eight books and more than 180 papers published in international journals and conferences.

http://orcid.org/0000-0002-9492-5818